

Physicochemical Characterization and *In Vitro* Hemolysis Evaluation of Silver Nanoparticles

Jonghoon Choi,^{*,†,1} Vytas Reipa,^{*} Victoria M. Hitchins,[†] Peter L. Goering,[†] and Richard A. Malinauskas^{†,2}

^{*}Biochemical Science Division, National Institute of Standards and Technology, Gaithersburg, Maryland 20899; and [†]Center for Devices and Radiological Health, U.S. Food and Drug Administration, Silver Spring, Maryland 20993

¹Present address: Department of Chemical Engineering, Massachusetts Institute of Technology, Cambridge, MA 02139.

²To whom correspondence should be addressed at Center for Devices and Radiological Health, Office of Science and Engineering Laboratories, U.S. Food and Drug Administration, 10903 New Hampshire Avenue, Building 62, Room 2108, Silver Spring, MD 20993-0002. Fax: (301) 796-9932.
E-mail: richard.malinauskas@fda.hhs.gov.

Received December 20, 2010; accepted January 1, 2011

Silver nanomaterials are increasingly being used as antimicrobial agents in medical devices. This study assessed the *in vitro* hemolytic potential of unbound silver particles in human blood to determine which physical and chemical particle properties contribute to mechanisms of red blood cell (RBC) damage. Four silver particle powders (two nano-sized and two micron-sized) were dispersed in water and characterized using transmission electron microscopy, dynamic light scattering, surface-enhanced Raman spectroscopy, and zeta potential measurement. Particle size and agglomeration were dependent on the suspension media. Under similar conditions to the hemolysis assay, with the particles added to phosphate buffered saline (PBS) and plasma, the size of the nanoparticles increased compared with particles suspended in water alone due to interaction with chloride ions and plasma proteins. To determine hemolysis response, aqueous particle suspensions were mixed with heparinized human blood diluted in PBS for 3.5 h at 37°C. Both nanoparticle preparations were significantly more hemolytic than micron-sized particles at equivalent mass concentrations > 220 µg/ml and at estimated surface area concentrations > 10 cm²/ml. The presence or absence of surface citrate on nanoparticles showed no significant difference in hemolysis. However, the aqueous nanoparticle preparations released significantly more silver ions than micron-sized particles, which correlated with increased hemolysis. Although significant size changes occurred to the silver particles due to interaction with media components, the higher level of *in vitro* hemolysis observed with nanoparticles compared with

micron-sized particles may be related to their greater surface area, increased silver ion release, and direct interaction with RBCs.

Key Words: silver nanoparticles; hemolysis; nanoparticle characterization; silver ions.

Silver has been used for centuries in health care delivery due to its antimicrobial and wound healing (anti-inflammatory) properties (Chaloupka *et al.*, 2010; Lansdown, 2010). Coatings generally comprised of silver salts or metallic silver have been used to prevent bacterial infections associated with medical devices, such as wound dressings, catheters, and orthopedic and cardiovascular implants, with different degrees of clinical efficacy (Wijnhoven *et al.*, 2009). Nanoscale silver has provided new opportunities for use in both consumer and biomedical applications due to its larger surface area-to-volume ratios and therefore greater reactivity (Chaloupka *et al.*, 2010; Chen and Schluesener, 2008; Wijnhoven *et al.*, 2009). Hence, silver nanoparticles may provide greater antimicrobial efficacy when used as coatings on cardiovascular and neurosurgical catheters and for wound and burn dressings (Chaloupka *et al.*, 2010; Wijnhoven *et al.*, 2009). Other biomedical uses of nanosilver include applications for drug delivery and bioimaging.

As the clinical use of silver nanoparticles increases, a better understanding of their safety when exposed to the bloodstream is needed. One of the fundamental tests in determining the safety of a blood-contacting medical material is to evaluate its hemolytic potential when exposed to blood *in vitro*. Hemolysis may occur if the red blood cell (RBC) membrane becomes compromised and hemoglobin is released, which may lead to adverse health effects (e.g., anemia, hypertension, renal toxicity) (Rother *et al.*, 2005). Although hemolysis tests have been conducted with various nanoparticles (Bosi *et al.*, 2004; Goodman *et al.*, 2004; Jovanovic *et al.*, 2006; Lee *et al.*, 2004), comparing results across studies are difficult due to variability

Disclaimer: The mention of commercial products, their sources, or their use in connection with material reported herein is not to be construed as either an actual or implied endorsement of such products by the Department of Health and Human Services. The conclusions and opinions expressed in this article are those of the authors and do not constitute Food and Drug Administration (FDA) policy, and the mention of any products and/or manufacturers does not imply FDA endorsement.

The authors certify that all research involving human subjects was done under full compliance with all government policies and the Helsinki Declaration

in the protocols for performing particle characterization and hemolysis testing (Dobrovolskaia and McNeil, 2007; Dobrovolskaia *et al.*, 2008; Fitzgerald *et al.*, 2011; Neun and Dobrovolskaia, 2011).

In this report, we characterized the physical and chemical properties of four different silver particle preparations and evaluated their hemolytic properties in dilute human blood using a test protocol described in the new consensus ASTM standard E2524-08—*Standard Test Method for Analysis of Hemolytic Properties of Nanoparticles* (ASTM International, West Conshohocken, PA, 2000) (Dobrovolskaia *et al.*, 2008). While identifying important limitations in the characterization and hemolysis test methods, we provide evidence that (1) the physicochemical properties of nano- and micron-sized silver particles are affected by the dispersing media and (2) silver nanoparticles are more hemolytic than silver micron-sized particles, which may be related to increased total surface area, silver ion release, or direct interaction between particles and cells.

MATERIALS AND METHODS

Silver particle preparations. Four separate silver particle dry powders were chosen to evaluate the effect of particle size (nano- and micron-sized) and surface chemistry (citrate stabilized or noncitrate) on hemolysis. Two suspensions of nanoscale silver particles (Ag-NP-S: “silver nanoparticles from Sigma,” labeled diameter $d < 100$ nm, citrate stabilized; Sigma-Aldrich, St Louis, MO, cat. #576832 and Ag-NP-N: “silver nanoparticles from NanoAmor,” $d \sim 35$ nm, cat. #0476JY; Nanostructured and Amorphous Materials, Inc., Houston, TX) at a concentration of 20 mg/ml were prepared by dispersion of the powders in deionized sterile water using an ultrasonic cleaner for 10 min. Dispersions were prepared in glass vials as the Ag-NP-S particles adhered to plastic vials. Similarly, two aqueous suspensions of microscale particles were also prepared from dry powders (Ag-MP: “silver microparticles,” $d = 2000$ – 3500 nm, cat. #327085; Sigma-Aldrich and Ag-MP-H: “silver microparticles heat treated,” which consisted of Ag-NP-S particles that had agglomerated after being dry heat treated (300°C , 10 min) to remove the surface-bound citrate). As the larger silver particles were not well dispersed and quickly sank in water, dilutions were prepared using large bore pipette tips to quickly withdraw aliquots from mixed samples. The three commercially available particles (Ag-NP-S, Ag-NP-N, and Ag-MP) had labeled silver purity of $\geq 99.5\%$.

Reagents. Cyanmethemoglobin reagent (CMH; Sigma-Aldrich) and hemoglobin standards (Stanbio Laboratory, Boerne, TX) were used as specified in the ASTM protocol to quantify the whole blood and plasma hemoglobin concentrations. $\text{Ca}^{2+}/\text{Mg}^{2+}$ -free Dulbecco’s phosphate-buffered saline (DPBS), polyethylene glycol (PEG), and Triton X-100 were purchased from Sigma-Aldrich.

Research donor human blood. Blood samples from healthy volunteers were collected into vials with heparin for anticoagulation according to Institutional Review Board approved protocols at the National Institutes of Health and the Food and Drug Administration. Blood from a different donor was used in each test on five separate days.

Particle characterization. Particle characterization was based on protocols developed by the Nanotechnology Characterization Laboratory (National Cancer Institute, Frederick, MD). Transmission electron microscopy (TEM) was performed using a JEM 2100 LaB₆ instrument (JEOL, Tokyo, Japan). A drop of silver particle suspension in water was deposited on a TEM carbon grid (Ted Pella, Inc., Redding, CA) and was allowed to dry at ambient

temperature. Elemental analysis was performed on the Ag-NP-S particles to confirm purity using energy-dispersive x-ray spectroscopy (INCAx-sight; Oxford Inc., Oxfordshire, UK) and a spectral database (Oxford Inc.).

Dynamic light scattering (DLS) and zeta potential measurements were performed using a ZetaPals (particle size analysis range of 0.6 nm–6 μm ; Brookhaven Instruments Corporation, Holtsville, NY) or a Zetasizer Nano instrument (range of 0.6 nm–6 μm ; Malvern Instruments, Worcestershire, UK). To reflect actual use in the hemolysis assay, the particle solutions were not filtered before performing the DLS analyses. The DLS measurements were based on particle number to determine the most abundant size population for comparative purposes (as opposed to using particle intensity as the main analysis parameter because this significantly skews the population results toward the largest particles). DLS particle size measurements were performed in water and other media to mimic the preparation and hemolysis assay conditions but without the presence of blood cells (i.e., aqueous particle solutions were exposed to DPBS for 3 min followed by DPBS-diluted blood plasma at the same concentration as used in the assay). Due to limitations in the DLS size analysis from time-dependent agglomeration, particle settling, and polydispersity when exposed to the different suspension media (i.e., water, DPBS, and DPBS with plasma), the DLS results should only be used to make qualitative comparisons between the particle suspensions.

Surface-enhanced Raman spectra were recorded with a Kaiser Holospec f1.8 spectrometer equipped with a thermoelectrically cooled CCD detector (Apogee, Inc., Roseville, CA). Samples were excited with a 647.1 nm Kr laser light (Innova 300; Coherent, Inc., Santa Clara, CA). Samples of the particle suspensions (200 μl) were prepared in a rectangular quartz cuvette (NSG Precision Cells, Inc., Farmingdale, NY), and spectra were acquired for 2–10 s with up to 150 mW of laser power on the sample. Spectra were processed using Grams (v. 7.02; Thermoelectron, Inc., Waltham, MA) and Sigmaplot (v. 9.0; Systat, Inc., San Jose, CA) software. Absorbance spectra of particles in water were recorded with an Ocean Optics Chem2000 fiber optic spectrophotometer (Ocean Optics, Dunedin, FL).

Silver ion release measurement in water. To determine silver ion release rate, multiple vials containing fresh particle suspensions in water were incubated in a water bath at 37°C for 210 min. At 30-min intervals, one vial for each particle type was removed from the bath and centrifuged at 10,000 g for 10 min to remove particles from the solution. The silver ion concentration was determined for each supernatant using an Orion 4-Star pH/ISE meter (Thermo Scientific, Beverly, MA) equipped with a silver/sulfide ion-selective electrode (Orion model# 9616BNWP; Thermo Scientific) that had been calibrated against a dilution series of AgNO_3 solutions. The free silver ion concentration in particle suspensions made in $\text{Ca}^{2+}/\text{Mg}^{2+}$ -free DPBS could not be measured with the ion-selective electrode because silver ions were binding with free chloride ions in DPBS to form insoluble precipitates.

Hemolysis assay. The detailed experimental procedure is outlined in the ASTM standard E2524-08 (*Standard Test Method for Analysis of Hemolytic Properties of Nanoparticles*) and is illustrated in Figure 1. Briefly, the total hemoglobin concentration of heparinized human whole blood was measured using the cyanmethemoglobin method based on a hemoglobin concentration standard curve at an absorbance wavelength of 540 nm. The blood was then diluted to a hemoglobin concentration of 10 mg/ml with $\text{Ca}^{2+}/\text{Mg}^{2+}$ -free DPBS. Particle samples at five different mass concentrations and positive and negative controls were analyzed in triplicate using blood from a different donor on each test day. Aliquots (100 μl) of either a nanoparticle or micron-particle suspension in water were added to microcentrifuge tubes, followed by the addition of 700 μl of $\text{Ca}^{2+}/\text{Mg}^{2+}$ -free DPBS. Within 3 min, diluted blood (100 μl) was added to each of the tubes. The small amount of water introduced with the particle samples did not induce hemolysis due to hypotonicity. The final mass concentrations of silver particles in the tubes ranged from 22 to 2200 $\mu\text{g}/\text{ml}$. The tubes were incubated in a 37°C water bath for 210 min with gentle inversion of the sample tubes every 30 min. Following the incubation, the tubes were centrifuged at $800 \times g$ for 15 min at room temperature. The supernatants were mixed in a 1:1 ratio with CMH reagent and analyzed at

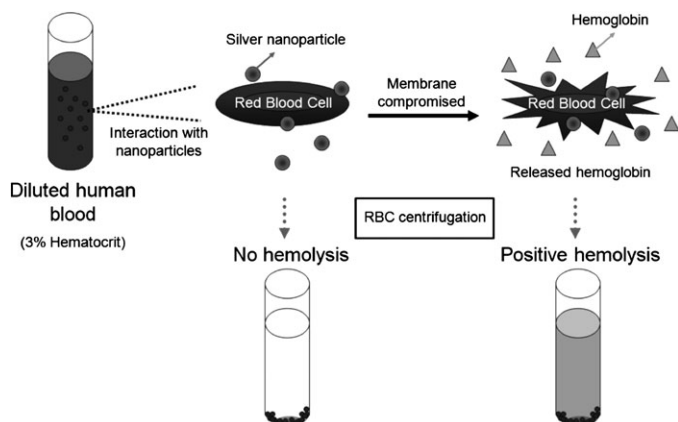


FIG. 1. *In vitro* hemolysis test of silver nanoparticles with human blood. Heparinized human blood was diluted with $\text{Ca}^{2+}/\text{Mg}^{2+}$ -free DPBS and added to solutions of silver nano- and micron-sized particles. After 3.5-h incubation in a 37°C water bath, the samples were centrifuged and the amount of hemoglobin released into the supernatant was quantified using the cyanmethemoglobin method as described in the “Materials and Methods” section.

540 nm. Sample absorbance was corrected for background interference (i.e., particles in DPBS without blood). The concentration of cell-free hemoglobin in each sample was assessed from the hemoglobin standard curve and by accounting for the 16-fold dilution factor for the samples and controls. Finally, the percent hemolysis was obtained by dividing each sample’s cell-free hemoglobin concentration by the total hemoglobin concentration (10 mg/ml). PEG (final concentration = 4.4%) was used as a negative control and Triton X-100 (final concentration = 1%) was used as a positive control.

Statistical analysis. For analyzing the hemolysis data, a two-way ANOVA with Bonferroni’s post-test was performed using GraphPad Prism version 5.0b for Mac OS X (GraphPad Software, San Diego, CA).

RESULTS

Characterization of Particles

Table 1 summarizes the particle size, dispersion, pH and zeta potential measurements in water, DPBS, and DPBS/plasma media. Differences in the sizes and shapes of the four commercial silver particle preparations in water were clearly visible in TEM images (Fig. 2). Ag-NP-S suspensions contained semi-spherical particles with a 30 nm mean diameter (Fig. 2A). The Ag-NP-N sample had a more heterogeneous size distribution than the Ag-NP-S sample with a mean particle diameter of about 100 nm (Fig. 2B). Interestingly, the mean diameter values were not consistent with the sizes specified by the particle vendors based on similar TEM measurements (Table 1). A possible reason for this discrepancy may be particle aggregation in water. Thus, the Ag-NP-S sample was closer to the manufacturer’s labeled size due to citrate coating, which prevented agglomeration due to the negative surface charges, whereas Ag-NP-N showed considerable agglomeration in the TEM images (Fig. 2B). Unlike nanoparticles, micron-sized silver particles (Ag-MP and Ag-MP-H) had a much wider size distribution range and included irregularly

shaped particles from a few tens of nanometers to several micrometers in diameter (Figs. 2C and 2D).

To complement the size analysis of dried particle suspensions performed by TEM, the hydrodynamic sizes of the particles in water were measured by DLS. The DLS-determined polydispersity index (PDI, which ranges from “0” for monodisperse samples to “1” for highly polydisperse samples) was the lowest for the two unfiltered nanoparticle samples ($\text{PDI} < 0.471$). The nano-sized particles also stayed dispersed in water for longer times (minutes to hours), whereas the micron-sized particles, especially Ag-MP, quickly settled and made the minutes-long DLS size measurements unreliable. Supplementary data (Supplementary Fig. 1) compare the size measurements for the nanoparticles by TEM and DLS.

Particle size and dispersion in different fluids were dependent on the initial particle size, the suspending media, and time (Table 1). When DPBS was added to the particles, they rapidly became larger and lighter in color due to reaction with chloride in the buffered media and the formation of AgCl. Visible precipitates of agglomerated particles formed for both of the micron-sized particles when exposed to DPBS. Conversely, when DPBS-diluted human plasma was added (at a $135\times$ dilution as used in the hemolysis assay), the particles stabilized and did not continue to increase in size over time but stayed dispersed much longer in the DPBS/plasma media versus in DPBS alone (Table 1). This phenomenon was further investigated by directly monitoring the physical state of the nanoparticles in both DPBS and DPBS-diluted blood plasma using optical absorbance and DLS measurements over time for up to 90 min (Table 1, Fig. 3). Incubation of both Ag-NP-S and Ag-NP-N nanoparticles in pure DPBS caused the formation of larger-sized and more polydisperse particles, as shown by the DLS data (Figs. 3A and 3C), and a pronounced decrease in particle solution absorbance (Figs. 3B and 3D). Decreases in the absorbance readings were due to aggregation and sedimentation of the particles, which made the solutions more transparent. The addition of dilute plasma to the DPBS inhibited these processes and noticeably stabilized Ag nanoparticles against corrosion and aggregation. This effect was observed for both citrate-stabilized (Ag-NP-S) and bare silver (Ag-NP-N) particles with only slight differences and is most likely attributable to the protein adsorption on the particle surface (also known as protein corona) (Dell’Orco *et al.*, 2010; Lundqvist *et al.*, 2008; Rucker *et al.*, 2009).

Based on the DLS analysis (Table 1), the Ag-NP-S particles increased in size from about 20 nm in water to 95 nm after incubation in DPBS (for 3 min) and increased in size to a range of 230–290 nm in DPBS/plasma (after 10 and 90 min). In contrast, the Ag-NP-N increased in size from 110 nm in water to 470 nm after incubation in DPBS (for 3 min); however, with the addition of plasma to the DPBS, the size decreased to a range of 335–385 nm for 10- and 90-min incubation. The Ag-MP-H averaged 860 nm in size in water but formed visible precipitates in DPBS. The addition of plasma to the DPBS resulted in

TABLE 1
Physical and Chemical Properties of Four Different Silver Particle Preparations in Different Media

Particles	Ag-NP-S	Ag-NP-N	Ag-MP	Ag-MP-H
Description	Citrate-stabilized nanoparticles from Sigma-Aldrich	Noncitrate nanoparticles from NanoAmor	Noncitrate micron particles from Sigma-Aldrich	Micron-sized particles (Ag-NP-S heated to remove surface citrate)
Size (nm)				
Product label	< 100	35	2000–3500	(none)
In water, DLS ^a	21 ± 6	111 ± 76 ^b	Precipitate ^c	860 ± 122 ^b
In water, TEM	30–50	50–300	800–3000	10–2000
In DPBS, DLS ^a (after 3 min)	94 ± 71	471 ± 323	Precipitate ^c	Precipitate ^c
In DPBS/plasma, DLS ^a (after 10 min)	287 ± 166	385 ± 187	Precipitate ^c	810 ± 119 ^b
In DPBS/plasma, DLS ^a (after 90 min)	227 ± 146	337 ± 99	Precipitate ^c	871 ± 140 ^b
Dispersion ^d				
Water	+++	++	–	–
DPBS	+++	+	–	–
DPBS/plasma	+++	++	–	–
pH				
Water	2.95	8.18	7.82	6.90
DPBS/plasma	6.89	7.7	7.40	7.40
Zeta potential (mV)				
Water	–41.8	–1.35	+ 1.28	+ 0.54
DPBS/plasma	+ 4.28	+ 2.40	+ 0.89	+ 0.20

^aDLS values based on number analysis to highlight the most abundant particle size for comparative purposes (mean ± peak width).

^bPDI ranged from 0.47 to 0.82 for all superscript-indicated DLS data. All other PDI values ranged from 0.21 to 0.38.

^cDLS measurements were unreliable for samples that had aggregated particles and visible precipitates.

^dDispersion of aqueous prepared particles in various media. (+++) Well-dispersed particles and (–) particles or agglomerates that quickly settled out of solution.

Ag-MP-H with a size range of 810–870 nm after 10- and 90-min incubation; as some precipitates were visible in the sample cuvette, these DLS measurements only represent the particles that stayed buoyant. Ag-MP formed precipitates in water, DPBS, and DPBS/plasma, which prevented making reliable DLS measurements of their size. However, the effect of plasma proteins on both of the micron-sized particles was to break apart large visible aggregates.

Analysis of chemical composition of the Ag-NP-S particles by energy emission x-ray spectroscopy showed peaks corresponding to silver (2.98 and 3.15 keV) (Supplementary Fig. 2). No other elements, except carbon (0.28 keV) and copper (8.0 and 8.9 keV), the latter originating from the TEM grid, were detected.

A citrate surface coating on the Ag-NP-S sample, but not on the heat-treated Ag-MP-H or native Ag-MP and Ag-NP-N particles, was confirmed by surface-enhanced Raman spectroscopy (SERS). In Figure 4, the Raman spectrum of pure citric acid is compared with the SERS spectra of all four colloids. Characteristic peaks (1390, 1089, 1016, 939, 829, and 791 cm⁻¹) from Ag-NP-S were attributed to citrates (Sulk *et al.*, 1999), although some peaks (1016 and 1089 cm⁻¹) were shifted, possibly as a result of surface interaction/orientation effects.

The net charge on the particles was assessed by measuring their electrophoretic mobility in water and the diluted DPBS/plasma solution (Table 1). The pH of Ag-NP-S particles in water was significantly lower (pH ~2.9) than in the other three preparations, which may be due to citrate deprotonation in water (Ag-NP-S had the strongest characteristic peaks for citric acid by SERS; Fig.4); as a result, the particles acquired a net negative charge as indicated by the zeta potential value (approximately –42 mV). However, the presence of the phosphate buffer in the DPBS/plasma solution neutralized the citrate effect on the pH and zeta potential for the Ag-NP-S preparation. The other three particle dispersions did not deviate considerably from neutral pH and surface charge when suspended in either media (Table 1).

In Vitro Hemolytic Property of Particles

The degree of hemolysis caused by silver particles exposed to dilute human blood for 3.5 h of incubation is shown in Figure 5. The percent hemolysis increased as a function of increasing mass concentration of particles in the DPBS/blood mixture. Among the four silver particle preparations, nano-sized particles (Ag-NP-S and Ag-NP-N) caused significantly greater levels of hemolysis ($p < 0.01$), exceeding 50% hemolysis for the particle

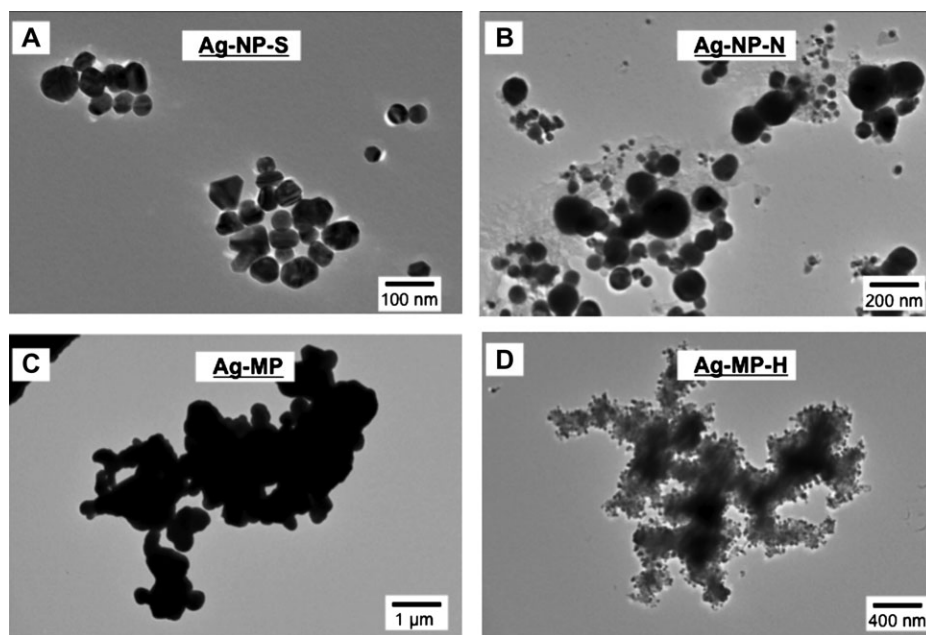


FIG. 2. TEM images of the four silver particle preparations (dried after being dispersed in water). (A) Silver nanoparticles obtained from Sigma-Aldrich (Ag-NP-S) had diameters in the range of 30–50 nm. (B) Silver nanoparticles obtained from Nanostructure and Amorphous Materials, Inc. (Ag-NP-N) showed a larger size distribution (50–300 nm in diameter) compared with Ag-NP-S. (C) Silver microparticles obtained from Sigma-Aldrich (Ag-MP) showed significant aggregations. (D) Micron-sized particles (Ag-MP-H) formed after heat treatment (300°C, 10 min) and agglomeration of Ag-NP-S particles.

concentrations at or above 700 $\mu\text{g}/\text{ml}$. In comparison, micron-sized silver particles (Ag-MP and Ag-MP-H) caused less than 12% hemolysis even at the highest concentration. According to the criterion in the ASTM E2524-08 standard, percent hemolysis $> 5\%$ indicates that the test material causes damage to RBCs; this criterion was exceeded at the particle concentration of 70 $\mu\text{g}/\text{ml}$ for the Ag-NP-N nanoparticles. Experiments included negative control (PEG) and positive control (Triton X-100) chemicals, and the results verified the performance of the hemolysis assay. Spectrophotometric analysis of the supernatants indicated that the silver particles did not shift the absorbance peaks of the hemoglobin released from the RBCs (data not shown).

Silver particle-induced hemolysis as a function of estimated surface area concentration, and particle number concentration, for each particle preparation (except Ag-MP) is shown in Figure 6 and Supplementary Figure 3, respectively. The total surface area concentration of the silver particles was calculated assuming a spherical shape and estimated from the mean hydrodynamic diameters measured in diluted DPBS/plasma after 90 min by DLS (Table 1). At surface area concentrations ranging from 1 to 10 cm^2/ml , hemolysis produced by Ag-NP-N progressively increased from approximately 10 to 50%. Hemolysis produced by Ag-NP-S was minimal at 1 cm^2/ml and progressively increased to 30% at 10 cm^2/ml . Ag-MP-H produced $< 10\%$ hemolysis at surface area concentrations of 10 cm^2/ml or less. At surface area concentrations $> 10 \text{ cm}^2/\text{ml}$, the two silver nanoparticle preparations produced a significant degree of hemolysis (50–80%) compared with the micron-sized silver particle (maximum hemolysis 10%).

Silver Ion Release Measurements

Silver ion release measurements were obtained at 30-min intervals from the Ag particles incubated in water at concentrations of 220 $\mu\text{g}/\text{ml}$ (Fig. 7). Particles were incubated in 37°C water for 3.5 h to simulate the conditions of the hemolysis assay. The rate of silver ion release from the nanoparticles (Ag-NP-S and Ag-NP-N) was linear over the first 150 min and was much higher (up to three orders of magnitude based on an equivalent mass concentration basis) than from the micron-sized particles (Ag-MP and Ag-MP-H). It was expected that the ion release would increase proportionally with particle surface area, and therefore, the nanoparticles would have a higher release rate than the micron-sized particles.

DISCUSSION

Silver nanoparticles are being increasingly utilized in blood-contacting biomedical applications and devices. As with any new technology, thorough preclinical evaluation is necessary to insure patient safety. For materials used in medical devices, this evaluation includes a two-step process: (1) physicochemical characterization of the material (i.e., nanoparticles in this case) and (2) biocompatibility assessment. As their unique size and composition affects their functionality, complete physicochemical descriptions of nanoparticles, both as dry particles and in their delivery media, are essential to fully characterize the material and to compare results between scientific studies. To improve the

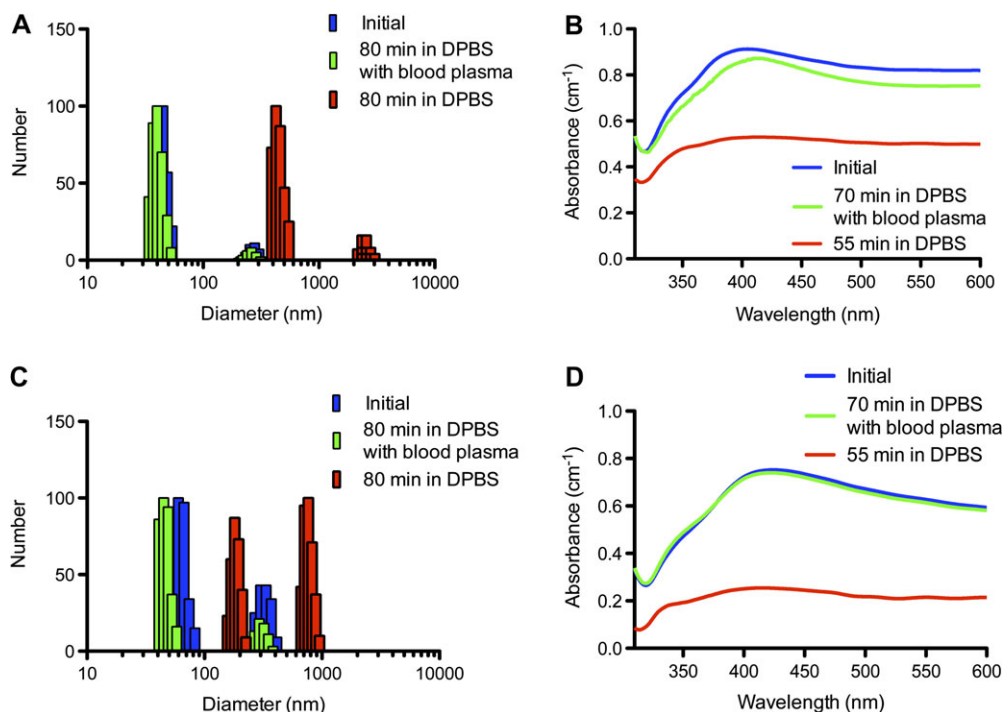


FIG. 3. Effect of DPBS and DPBS-diluted blood plasma on particle size distribution measured by DLS (A and C) and absorbance spectra (B and D) of two Ag nanoparticle preparations (A and B: Ag-NP-S and C and D: Ag-NP-N) over predetermined time points (DLS for 80 min; absorbance spectra for 70 min in DPBS-diluted blood plasma and for 55 min in DPBS). Initial time point ($t = 0$ min) was when particles were mixed in DPBS with 135 \times diluted human blood plasma.

biocompatibility evaluation of nanoparticles, the fundamental testing standard for assessing the hemolytic potential of blood-contacting materials (ASTM F756: *Standard Practice for Assessment of Hemolytic Properties of Materials*) was modified. The new ASTM E2524-08 standard was developed to accommodate hemolysis testing of small quantities of nanomaterials in human blood (Dobrovolskaia *et al.*, 2008). The main objectives of the present study were (1) to apply the

ASTM E2524-08 standard to determine the hemolytic properties of silver particles on human RBCs, (2) to relate the hemolysis results to the physicochemical characteristics of the particles (i.e., nano- or micron-sized, citrate stabilized, or noncitrate), and (3) to identify important limitations of the characterization and hemolysis test methods.

Physicochemical Characterization: Particle Diameter Measurements

Four silver particle powders were divided into two primary size domains: nano and micro. By conventional definition, Ag-NP-S and Ag-NP-N were nano-sized labeled particles ($d < 100$ nm), whereas Ag-MP and Ag-MP-H were micron-sized particles ($d > 1$ μ m). The silver nanoparticles were well dispersed in water and did not show significant agglomeration or morphological variations in TEM images. There was some discrepancy in mean particle size between that reported on the product labels (using TEM to measure suspended particles that were allowed to dry) compared with the values that we measured by both TEM and DLS (Table 1). These discrepancies may be due to differences in both preparation and the inherent limitations of nanoparticle sizing methods and emphasize the necessity to apply multiple techniques for determining particle sizes in polydisperse batches (Brown *et al.*, 2010; Lee *et al.*, 2004; Murdock *et al.*, 2008; Powers *et al.*, 2006). Although TEM can serve as a tool to capture the size of each individual particle, it is limited in that it can only measure particles after they have been suspended and then dried, it requires

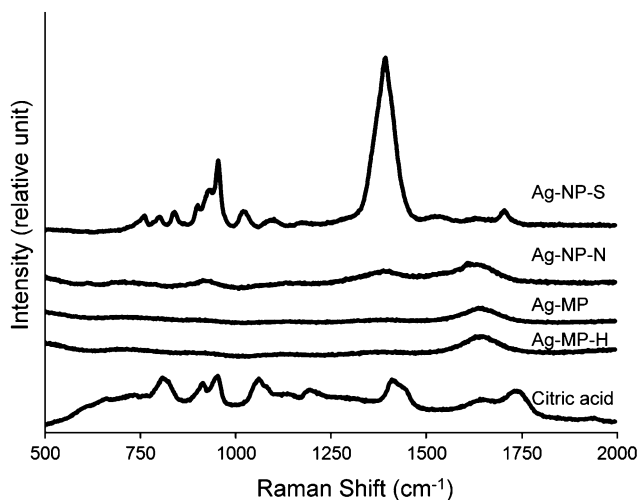


FIG. 4. Raman spectra of Ag-NP-S, Ag-NP-N, Ag-MP, and heat-treated Ag-NP-S particle (i.e., Ag-MP-H) colloidal solutions compared with citric acid (C₆H₈O₇). Surface citrate was only detected on the Ag-NP-S particles.

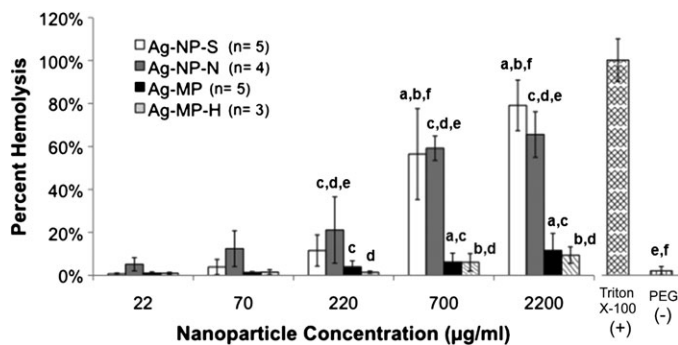


FIG. 5. *In vitro* hemolysis test results for diluted human blood exposed to silver particles. After 3.5-h incubation in a 37°C water bath, the amount of hemoglobin released into the supernatant was quantified using the cyanmethemoglobin method as described in the “Materials and Methods” section. PEG was used as a negative control (–) and Triton X-100 was used as a positive control (+) on each test day. Values represent mean \pm SD from experiments performed in triplicate on up to five separate days (e.g., $n = 5$ days in legend). For each concentration, hemolysis means with the same letter (a–f) were significantly different from each other. For example, the hemolysis result of Ag-NP-N at 220 $\mu\text{g}/\text{ml}$ (c, d, e) is significantly different from Ag-MP at 220 $\mu\text{g}/\text{ml}$ (c), Ag-MP-H at 220 $\mu\text{g}/\text{ml}$ (d), Ag-NP-N at 700 $\mu\text{g}/\text{ml}$ (c, d, e), and the negative control (e) at a statistical level of $p < 0.01$. Hemolysis values were not statistically different between the four particles at the concentrations of 22 and 70 $\mu\text{g}/\text{ml}$. Hemolysis levels for all particle concentrations were significantly different from the positive control at $p < 0.001$; however, the statistical significance is not shown on the figure.

measurements of many different particle regions to appropriately represent the entire particle batch, and complex geometries of particles or agglomerates may make characterization difficult. The measurements may also be affected by the solvent used to disperse the particles prior to drying for TEM analysis.

Although DLS is performed in solutions, the suspending media and how the particle sample was mixed (i.e., sonication intensity and exposure time) and prefiltered can significantly affect the particle hydrodynamic size analysis. Moreover, particle agglomeration and time-dependent sedimentation of large (i.e., $d > 100$ nm) and dense silver particles may affect the DLS measurement reliability even during the short measurement time period (2–5 min). DLS measurements of highly polydispersed particle solutions are also dependent on the main analysis parameter (i.e., intensity, volume, number). In an intensity-based DLS analysis of a polydisperse particle sample, smaller particles are underrepresented due to weaker light scattering and particle shape effects (Grabowski and Morrison, 1983; Herb *et al.*, 1987; Zook *et al.*, 2010). For this reason, we utilized a number-based DLS analysis to highlight the most abundant particle size population so that we could make limited comparisons between the different particles, especially because the particles were not prefiltered and the effect of media on nanoparticle size, agglomeration, and polydispersity was significant. Murdock *et al.* (2008) similarly reported changes in the size and polydispersity of different nanoparticles when mixed in water, cell media, and cell media with serum proteins, with high PDI values ranging from 0.835 to 1 for uncoated 80-nm silver particles. Due to the time- and

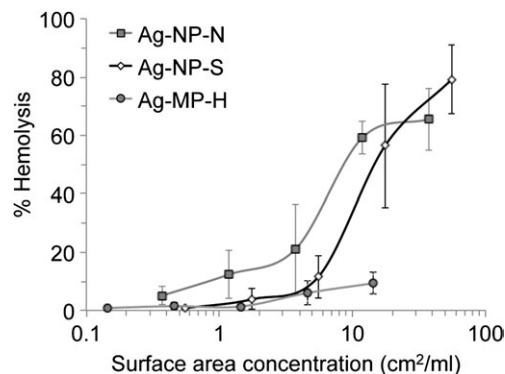


FIG. 6. Percent hemolysis versus total particle surface area concentration. Hemolysis assay results from Figure 5 were replotted against the estimated available exposed surface area of three silver particles measured by DLS in DPBS/plasma. (Total sample volume of 0.9 ml).

media-dependent changes in the silver particles and their high polydispersities, the DLS measurements in this study could only provide estimates of the particle size distributions.

In general, there was an increase in particle size and/or agglomeration, either by DLS measurement or visually, when aqueous particle suspensions were mixed with DPBS media due to reaction with chloride ions and the presumable formation of poorly soluble silver chloride. However, the effect of dilute plasma proteins in the media acted to stabilize the particles, break apart large agglomerates, and increase their dispersion. This protein-coating effect has been used to control the formation of stable agglomerates of silver nanoparticles in biological media so that they remain well dispersed for days (Zook *et al.*, 2010).

Particle Size, Surface Area, Silver Ion Release, and Hemolysis

Our data suggest that particle size and surface area are key factors that affect hemolysis. A distinct increase in the hemolytic properties of nano-sized silver particles compared with the micron-sized particles at equivalent mass concentrations was observed (Fig. 5). The percent hemolysis (corrected using the negative control background value) of the Ag-NP-N particles exceeded the 5% reportable blood damage criterion listed in the ASTM E2524-08 standard at a mass concentration of 70 $\mu\text{g}/\text{ml}$, whereas hemolysis for the micron-sized particles did not exceed this threshold until the particle concentration was 2200 $\mu\text{g}/\text{ml}$. Our hemolysis results are consistent with those recently reported by Zook *et al.* (2010) that showed hemolysis caused by large agglomerates of protein-stabilized silver particles (1100 and 1400 nm in size) was significantly less than for smaller agglomerates (43, 190, and 490 nm in size). Although the nanoparticles increased in size due to interaction with DPBS and plasma proteins during the hemolysis assay in the current study (Table 1), we hypothesize that a larger total surface area afforded by the nanoparticles, particularly at the highest concentrations, provided a greater probability of interaction between unbound

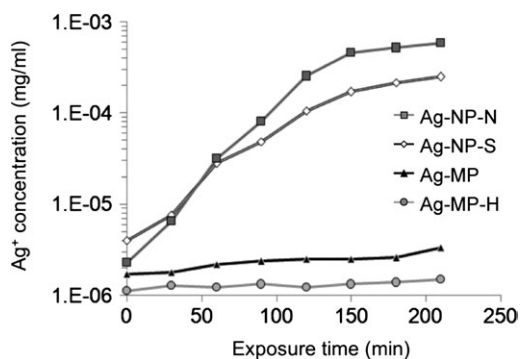


FIG. 7. Ag^+ ion release measurements from silver particles suspended in water at a starting mass concentration of 220 $\mu\text{g}/\text{ml}$ for each Ag sample. Particles were incubated in water at 37°C for 3.5 h with Ag ion concentration sampled every 30 min using an ion-selective electrode.

silver ions, metallic silver particles, and the RBC membrane that led to hemolysis.

The mechanisms by which silver nanoparticles may induce hemolysis in erythrocytes under physiological conditions have not been completely elucidated. In contact with body fluids, metallic silver ionizes and releases Ag^+ as a function of the particle surface area (Lansdown, 2010). Low concentrations of Ag^+ ions *in vitro* are known to cause RBC hemolysis (Ballinger *et al.*, 1982). Silver ions can also incite suicidal RBC death as characterized by decreased ATP content and phosphatidylserine exposure on the RBC surface (Sopjani *et al.*, 2009). However, silver ions quickly bind with anionic ligands in biologic media including chloride (Cl^-), inorganic sulfide, and thiols ($-\text{SH}$) (e.g., within albumin proteins) (Liu *et al.*, 2010). Although this binding acts to theoretically reduce the bioavailability of Ag^+ for damaging cells (Christensen *et al.*, 2010; Lansdown, 2010), it may also cause structural and functional changes to proteins and important antioxidants (Johnston *et al.*, 2010). Garner *et al.* (1994) observed a large depletion of the RBC intracellular antioxidant glutathione when erythrocytes were exposed to 30 nm silver colloids. Ballinger *et al.* (1982) demonstrated that Ag^+ ions could remain bioavailable by using sulphadimidine as a carrier, which resulted in significant hemolysis even in the presence of chloride ions. Hence, due to the complex reactivity of silver ions with biologic components, future mechanistic investigations might consider silver interactions with RBC transmembrane proteins, such as anion exchanger 1 (a transporter of chloride and bicarbonate across the plasma membrane) and glycophorins (de Oliveira and Saldanha, 2010; Tanner, 1997), as well as with cellular antioxidants (e.g., glutathione) (Garner *et al.*, 1994).

It is unclear whether nanosilver toxicity to cells is due to the rate of release of free silver ions, the overall silver ion concentration, direct cellular interaction with particles, or a combination of these events (Christensen *et al.*, 2010; Johnston *et al.*, 2010; Lansdown, 2010; Wijnhoven *et al.*, 2009). If silver ion generation was the primary factor for hemolysis, then the total particle surface area concentration versus hemolysis plots (Fig. 6) should have been similar for

each particle (assuming silver ion release is proportional to surface area). However, our data show that smaller particles were more hemolytic than micron-sized ones when compared at surface area concentrations greater than about 10 cm^2/ml (Fig. 6), which implies that another mechanism contributed to the hemolysis by the nanoparticles.

Although high silver ion release rates and concentrations were recorded for nanoparticles dispersed in water in the present study (Fig. 7), most likely due to an increased total surface area, we assume that smaller amounts of free silver ions were available in DPBS-plasma solutions during the hemolysis testing. This assumption is based on binding of Ag^+ ions with free chloride ions to form AgCl , decreased surface area due to particle agglomeration, and the formation of a protein corona on the particles. As these mechanisms limit the amount of available unbound Ag^+ ions in the DPBS-blood media that may damage the RBCs, hemolysis due to direct particle interaction with the RBC membrane should also be considered as a potential damage mechanism. For example, nanoparticles in direct contact with RBCs could continuously release silver ions locally that may not be detoxified by binding to plasma chloride or proteins. Moreover, nonspecific uptake of particles by RBCs was found to occur by an unknown pathway that was dependent on particle size (only particles less than or equal to 200 nm diameter entered the RBCs) and not governed by the particle material type or charge (Rothen-Rutishauser *et al.*, 2006). Thus, the substantive levels of hemolysis from nanoparticles observed in the present study may be related to silver ion generation, direct particle interaction with the RBC membrane, and particle uptake by RBCs; however, it is not clear as to the relative contribution of each.

Nanoparticle Surface Chemistry

The role of the surface chemical structure on the rate of silver particle dissolution, i.e., Ag^+ release, in aqueous media is not completely established. Silver rapidly oxidizes when exposed to oxygenated aqueous solutions; however, the presence of citrate in such solutions was found to significantly retard silver nanowire corrosion (Stoermer *et al.*, 2005). We observed that the citrate surface coating (qualitatively assessed using SERS as shown in Fig. 4) reduced the Ag^+ ion release rate of the smaller Ag-NP-S particles relative to the noncitrate Ag-NP-N particles. The citrate coating on the Ag-NP-S particles may have passivated the particle surface, by providing a mild reducing environment, and protected against particle corrosion that may have resulted in the lower silver ion release in water (Fig. 7).

Citrate is the conjugate base of citric acid, which is a popular reducing agent used in silver and gold production, and provides a negatively charged surface moiety that stabilizes nanoparticle colloids through Coulombic repulsion. The citrate-stabilized Ag-NP-S nanoparticles suspended in water acquired a significant negative charge (zeta potential = -41.8 mV) and acidified the aqueous solution ($\text{pH} = 2.95$). In order to elucidate the role of the citrate surface coating on hemolysis, we used a thermal

treatment to remove the coating from the dry Ag-NP-S particles, but we did not anticipate that aggregation would result in formation of micron-sized particles (Ag-MP-H). Hence, we cannot conclude that the citrate coating was the only factor responsible for the increase in hemolysis with Ag-NP-S particles compared with Ag-MP-H due to the significant differences in particle sizes. In comparing the nano-sized particles, it was found that each population had similar pH and zeta potentials when diluted in a DPBS/blood solution regardless of the degree of citrate coating on each particle (Table 1). Furthermore, no significant differences in hemolysis levels between the two nano-sized particles argues in favor of particle size as a stronger determinant of hemolysis rather than initial surface chemical properties.

Serum proteins have been shown to have a significant effect on particle toxicity, possibly due to changes in agglomeration or surface chemistry (Murdock *et al.*, 2008). In our study, the blood plasma proteins provided a stabilizing effect against nanoparticle agglomeration, as also seen by others (Dell'Orco *et al.*, 2010; Lundqvist *et al.*, 2008; Murdock *et al.*, 2008; Nel *et al.*, 2009). In spite of the protein coating on the silver particles, hemolysis still occurred. Zook *et al.* (2010) similarly reported that albumin-coated silver nanoparticles induced hemolysis but noted that increasing the protein concentration decreased hemolytic activity. Further studies are needed to explore how protein interactions with nanoparticles affect their physicochemical and biological properties.

Limitations of the Current Study and the ASTM E2524-08 Standard

Although the new ASTM E2524-08 consensus standard for assessing hemolytic properties of unbound nanoparticles provides a detailed testing protocol, this study revealed some important aspects of the methodology that could impact the test results. It is expected that most nanoparticles would be well dispersed and stabilized in a physiologic solution before undergoing the hemolysis testing, but this was not the case in our study as dry powder silver particles required initial preparation in water because they aggregated quickly in DPBS. Also, as DPBS was added to the silver particle in water suspensions prior to adding the blood (per the standard), this may have decreased the sensitivity and reliability of the hemolysis assay due to particle agglomeration and the formation of AgCl. The addition of plasma proteins mitigated agglomeration and improved particle dispersion. Accommodation needs to be made for particles prepared in media other than DPBS alone, which may be used in the testing or introduced intravenously (e.g., 5% dextrose in water). When characterizing, testing, and comparing results for nanoparticles, the current study reinforces the importance of the effect of serum proteins on particle size, dispersion, and cellular toxicity (Murdock *et al.*, 2008; Zook *et al.*, 2010).

Particle size and density may affect the hemolysis assay by impacting exposure of the diluted RBCs to the particles during the incubation period. The standard suggests two general methods for mixing samples while they are being incubated at

37°C (i.e., using a tube rotator in an incubator for continuous mixing or rotating tubes placed in a water bath by hand every 30 min). We used the latter method in our study, although the settling rates for the RBCs and the different size silver particles were not the same. For different particle sizes and types, it should be determined if the mixing method influences the hemolysis results.

Other mechanisms of particle interference with the assay have also been identified (Dobrovolskaia *et al.*, 2008); coagulation of blood around particles can prevent RBC particle interaction and hemolysis, particles can adsorb hemoglobin so that it is removed during centrifugation causing an underestimate of the hemolysis level, nanoparticles may not be completely removed during the centrifugation step, and light absorbance of the retained particles may interfere by being near the assay wavelength of 540 nm. Visible observation of the particles during all phases of the testing is encouraged to identify potential problems. In summary, although the ASTM E2524-08 standard is an important first step for screening unbound nanoparticles for their hemolytic potential, researchers must be aware of the possible pitfalls and limitations which may affect the test protocol and results for different particles. It would be beneficial to identify nanoparticle-based positive and negative controls for use in the assay that could be evaluated through an interlaboratory study.

We found that size characterization was especially challenging in this study as the silver particles reacted with chloride in the DPBS medium used in the hemolysis assay and affected the reliability of the DLS measurements. However, although hydrodynamic particle size increased in DPBS medium alone, dilute plasma present in the media had a stabilizing effect on particle size. Even with the many limitations, the results of this study were reproducible and showed the dependence of silver particle size and mass concentration on hemolysis; silver nanoparticles with diameters around 100 nm in water were significantly more hemolytic than micron-sized silver particles. No statistically significant effect on hemolysis of citrate on the Ag particle surface was observed. A concentration-dependent increase in hemolysis was observed with marked hemolysis (> 10%) occurring at nanoparticle concentrations at or above 220 µg/ml (equivalent to around 4 cm²/ml in total particle surface area concentration). Although measured in water and not in a biologic media, significantly higher Ag⁺ ion release rates were found for silver nanoparticle suspensions compared with micron-sized preparations at similar mass concentrations. The mechanism of nanosilver-induced hemolysis may be related to the rate of release of free silver ions, the total amount of silver ions released, direct interaction between particles and RBCs, or a combination of these factors; however, the relative contribution of each of these events cannot be determined from this study. Our *in vitro* hemolysis results suggest that commercially available blood-contacting medical devices containing silver nanoparticles, whether as free particles or bound in a matrix, should be carefully evaluated for their hemolytic potential.

SUPPLEMENTARY DATA

Supplementary data are available online at <http://toxsci.oxfordjournals.org/>.

FUNDING

This work was supported by the Oak Ridge Institute for Science and Education through a fellowship from the United States Food and Drug Administration to JC.

ACKNOWLEDGMENTS

The authors would like to thank Dr Nam Sun Wang (Department of Chemical and Biomolecular Engineering) and the Maryland Nanocenter at the University of Maryland for electron microscopy resources and the Research Blood Donor program at the National Institutes of Health Blood Bank. We also acknowledge Drs Benita Dair and Qin Zhang at the FDA for invaluable discussions and help on the DLS, zeta potential, and silver ion content measurements and Dr Parag Aggarwal for review and suggestions on the manuscript.

REFERENCES

- Ballinger, P. M., Brown, B. S., Griffin, M. M., and Steven, F. S. (1982). Evidence for carriage of silver by sulphadimidine: haemolysis of human erythrocytes. *Br. J. Pharmacol.* **77**, 141–145.
- Bosi, S., Feruglio, L., Da Ros, T., Spalluto, G., Gregoretti, B., Terdoslavich, M., Decorti, G., Passamonti, S., Moro, S., and Prato, M. (2004). Hemolytic effects of water-soluble fullerene derivatives. *J. Med. Chem.* **47**, 6711–6715.
- Brown, S. C., Palazuelos, M., Sharma, P., Powers, K. W., Roberts, S. M., Grobmyer, S. R., and Moudgil, B. M. (2010). Nanoparticle characterization for cancer nanotechnology and other biological applications. *Methods Mol. Biol.* **624**, 39–65.
- Chaloupka, K., Malam, Y., and Seifalian, A. M. (2010). Nanosilver as a new generation of nanoparticle in biomedical applications. *Trends Biotechnol.* **28**, 580–588.
- Chen, X., and Schluesener, H. J. (2008). Nanosilver: a nanoparticle in medical application. *Toxicol. Lett.* **176**, 1–12.
- Christensen, F. M., Johnston, H. J., Stone, V., Aitken, R. J., Hankin, S., Peters, S., and Aschberger, K. (2010). Nano-silver—feasibility and challenges for human health risk assessment based on open literature. *Nanotoxicology* **4**, 284–295.
- de Oliveira, S., and Saldanha, C. (2010). An overview about erythrocyte membrane. *Clin. Hemorheol. Microcirc.* **44**, 63–74.
- Dell'Orco, D., Lundqvist, M., Oslakovic, C., Cedervall, T., and Linse, S. (2010). Modeling the time evolution of the nanoparticle-protein corona in a body fluid. *PLoS One* **5**, e10949.
- DiVincenzo, G. D., Giordano, C. J., and Schriever, L. S. (1985). Biologic monitoring of workers exposed to silver. *Int. Arch. Occup. Environ. Health* **56**, 207–215.
- Dobrovolskaia, M. A., Clogston, J. D., Neun, B. W., Hall, J. B., Patri, A. K., and McNeil, S. E. (2008). Method for analysis of nanoparticle hemolytic properties in vitro. *Nano Lett.* **8**, 2180–2187.
- Dobrovolskaia, M. A. and McNeil, S. E. (2007). Immunological properties of engineered nanomaterials. *Nat. Nanotechnol.* **2**, 469–478.
- Fitzgerald, K. T., Holladay, C. A., McCarthy, C., Power, K. A., Pandit, A., and Gallagher, W. M. (2011). Standardization of models and methods used to assess nanoparticles in cardiovascular applications. *Small* **7**, 705–717.
- Garner, M., Reglinski, J., Smith, W. E., and Stewart, M. J. (1994). The interaction of colloidal metals with erythrocytes. *J. Inorg. Biochem.* **56**, 283–290.
- Goodman, C. M., McCusker, C. D., Yilmaz, T., and Rotello, V. M. (2004). Toxicity of gold nanoparticles functionalized with cationic and anionic side chains. *Bioconjug. Chem.* **15**, 897–900.
- Grabowski, E., and Morrison, I. (1983). Particle size distributions from analysis of quasi-elastic light scattering data. In *Measurements of Suspended Particles by Quasi-Elastic Light Scattering* (B. Dahneke, Ed.), pp. 105–120, Wiley-Interscience, New York, NY.
- Herb, C. A., Berger, E. J., Chang, K., Morrison, I. D., and Grabowski, E. F. (1987). *Using Quasi-Elastic Light Scattering to Study Particle Size Distributions in Submicrometer Emulsion Systems. Particle Size Distribution (ACS Symposium Series, 332: American Chemical Society)*, 89–104.
- Johnston, H. J., Hutchison, G., Christensen, F. M., Peters, S., Hankin, S., and Stone, V. (2010). A review of the in vivo and in vitro toxicity of silver and gold particulates: particle attributes and biological mechanisms responsible for the observed toxicity. *Crit. Rev. Toxicol.* **40**, 328–346.
- Jovanovic, A. V., Flint, J. A., Varshney, M., Morey, T. E., Dennis, D. M., and Duran, R. S. (2006). Surface modification of silica core-shell nanocapsules: biomedical implications. *Biomacromolecules* **7**, 945–949.
- Lansdown, A. B. G. (2010). A pharmacological and toxicological profile of silver as an antimicrobial agent in medical devices. *Adv. Pharmacol. Sci.* **2010**, 1–16.
- Lee, D. W., Powers, K., and Baney, R. (2004). Physicochemical properties and blood compatibility of acylated chitosan nanoparticles. *Carbohydr. Polym.* **58**, 371–377.
- Liu, J., Sonshine, D. A., Shervani, S., and Hurt, R. H. (2010). Controlled release of biologically active silver from nanosilver surfaces. *ACS Nano* **4**, 6903–6913.
- Lundqvist, M., Stigler, J., Elia, G., Lynch, I., Cedervall, T., and Dawson, K. A. (2008). Nanoparticle size and surface properties determine the protein corona with possible implications for biological impacts. *Proc. Natl. Acad. Sci. U.S.A.* **105**, 14265–14270.
- Murdoch, R. C., Braydich-Stolle, L., Schrand, A. M., Schlager, J. J., and Hussain, S. M. (2008). Characterization of nanomaterial dispersion in solution prior to in vitro exposure using dynamic light scattering technique. *Toxicol. Sci.* **101**, 239–253.
- Nel, A. E., Madler, L., Velegol, D., Xia, T., Hoek, E. M., Somasundaran, P., Klaessig, F., Castranova, V., and Thompson, M. (2009). Understanding biophysicochemical interactions at the nano-bio interface. *Nat. Mater.* **8**, 543–557.
- Neun, B. W., and Dobrovolskaia, M. A. (2011). Method for analysis of nanoparticle hemolytic properties in vitro. In *Characterization of Nanoparticles Intended for Drug, Delivery, Methods in Molecular Biology* (S. E. McNeil, Ed.), Vol. 697, pp. 215–224. Springer Science+Business Media, LLC, New York, NY.
- Powers, K. W., Brown, S. C., Krishna, V. B., Wasdo, S. C., Moudgil, B. M., and Roberts, S. M. (2006). Research strategies for safety evaluation of nanomaterials. Part VI. Characterization of nanoscale particles for toxicological evaluation. *Toxicol. Sci.* **90**, 296–303.
- Rocker, C., Potzl, M., Zhang, F., Parak, W. J., and Nienhaus, G. U. (2009). A quantitative fluorescence study of protein monolayer formation on colloidal nanoparticles. *Nat. Nanotechnol.* **4**, 577–580.
- Rothen-Rutishauser, B. M., Schürch, S., Haenni, B., Kapp, N., and Gehr, P. (2006). Interaction of fine particles and nanoparticles with red blood cells visualized with advanced microscopic techniques. *Environ. Sci. Technol.* **40**, 4353–4359.

- Rother, R. P., Bell, L., Hillmen, P., and Gladwin, M. T. (2005). The clinical sequelae of intravascular hemolysis and extracellular plasma hemoglobin: a novel mechanism of human disease. *JAMA* **293**, 1653–1662.
- Sopjani, M., Foller, M., Haendeler, J., Gotz, F., and Lanf, F. (2009). Silver ion-induced suicidal erythrocyte death. *J. Appl. Toxicol.* **29**, 531–536.
- Stoermer, R. L., Sioss, J. A., and Keating, C. D. (2005). Stabilization of silver metal in citrate buffer: barcoded nanowires and their bioconjugates. *Chem. Mater.* **17**, 4356–4361.
- Sulk, R., Chan, C., Guicheteau, J., Gomez, C., Heyns, J. B. B., Corcoran, R., and Carron, K. (1999). Surface-enhanced Raman assays (SERA): measurement of bilirubin and salicylate. *J. Raman Spectrosc.* **30**, 853–859.
- Tanner, M. J. (1997). The structure and function of band 3 (AE1): recent developments (review). *Mol. Membr. Biol.* **14**, 155–165.
- Wijnhoven, S. W. P., Peijnenburg, W. J. G. M., Herberts, C. A., Hagens, W. I., Oomen, A. G., Heugens, E. H. W., Roszek, B., Bisschops, J., Gosens, I., and Van De Meent, D. (2009). Nano-silver—a review of available data and knowledge gaps in human and environmental risk assessment. *Nanotoxicology* **3**, 109–138.
- Zook, J. M., Maccuspie, R. I., Locascio, L. E., Halter, M. D., and Elliott, J. T. (2010). Stable nanoparticle aggregates/agglomerates of different sizes and the effect of their size on hemolytic cytotoxicity. *Nanotoxicology* Advance Access published on December 13, 2010. doi:10.3109/17435390.2010.536615.